Plant Physiol. (1998) 116: 991–1001

Spatial and Temporal Analyses of Expansion and Cell Cycle in Sunflower Leaves[1]

A Common Pattern of Development for All Zones of a Leaf and Different Leaves of a Plant

Christine Granier and François Tardieu*

Institut National de la Recherche Agronomique, Laboratoire d'Ecophysiologie des Plantes sous Stress Environnementaux, 2 Place Viala, 34060 Montpellier, France

We have investigated the spatial distributions of expansion and cell cycle in sunflower (*Helianthus annuus* L.) leaves located at two positions on the stem, from leaf initiation to the end of expansion. Relative expansion rate (*RER*) was analyzed by following the deformation of a grid drawn on the lamina; relative division rate (*RDR*) and flow-cytometry data were obtained in four zones perpendicular to the midrib. Calculations for determining in situ durations of the cell cycle and of S-G2-M in the epidermis are proposed. Area and cell number of a given leaf zone increased exponentially during the first two-thirds of the development duration. *RER* and *RDR* were constant and similar in all zones of a leaf and in all studied leaves during this period. Reduction in *RER* occurred afterward with a tip-to-base gradient and lagged behind that of *RDR* by 4 to 5 d in all zones. After a long period of constancy, cell-cycle duration increased rapidly and simultaneously within a leaf zone, with cells blocked in the G0-G1 phase of the cycle. Cells that began their cycle after the end of the period with exponential increase in cell number could not finish it, suggesting that they abruptly lost their competence to cross a critical step of the cycle. Differences in area and in cell number among zones of a leaf and among leaves of a plant essentially depended on the timing of two events, cessation of exponential expansion and of exponential division.

Analysis of the genetic controls of leaf shape, cell division, and tissue expansion has progressed lately with the characterization of mutants with altered leaf development, especially in dicot species such as *Nicotiana tabacum* (Hemerly et al., 1995; Sato et al., 1996) or *Arabidopsis thaliana* (Tsuge et al., 1996; Van Lijsebettens et al., 1996). However, quantitative studies of these processes are still needed, in dicot species, for analysis of the consequences of mutations, as well as those of environmental conditions (Yegappan et al., 1980; Lecoeur et al., 1995). The framework of growth analysis, which has been developed in recent years, has essentially been applied to organs with monodimensional growth, such as roots or monocot leaves (Gandar and Hall, 1988; Silk, 1992; Peters and Bernstein, 1997). In such cases cells are continuously produced in the meristematic region near the leaf base (or root apex) and are moved from the meristem by subsequent cell production and elongation (Fraser et al., 1990; Skinner and Nelson, 1994). It takes from 8 h to 3 d for a new cell to become mature, i.e. the time for the cell to cross the zones of cell division and of expansion (Sharp et al., 1988; Ben Haj Salah and Tardieu, 1995). Conditions of steady state in the expanding zone can be easily obtained during this short time, thereby allowing the deduction of temporal from spatial patterns.

The development of dicot leaves is bidimensional and occurs over a considerably longer time than that in the monodimensional case. Cell division and expansion occur over weeks (versus days in monocot leaves) and overlap temporally in all zones of a leaf. During the first weeks of leaf development, expansion is slow (Maksymowych, 1973), cell division takes place in the whole leaf, and it stops before the end of leaf expansion (Milthorpe and Newton, 1963; Yegappan et al., 1980; Lecoeur et al., 1995). As in the case of monocot leaves, gradients of cell development exist from the base to the tip of the leaf, involving nonuniformity in the local expansion rate (Avery, 1933; Saurer and Possingham, 1970; Poethig and Sussex, 1985; Wolf et al., 1986). However, temporal processes cannot be deduced from the spatial pattern in dicot leaves (Eulerian specification); therefore, temporal and spatial analyses of leaf expansion and cell division must be carried out over the whole duration of leaf development (Lagrangian specification).

Cell division and cell expansion are frequently considered the two processes of interest in growth analysis. However, Green (1976) suggested that only tissue expansion should be considered as volumetric growth, whereas cell size should be considered the consequence of two independent processes, tissue expansion and cell division. Consistently, the cell division rate has been shown to be regulated independently of the tissue expansion rate in some cases

[1] This work was supported by grants from the Institut National de la Recherche Agronomique and the Centre Technique Interprofessionnel des Oléagineux Métropolitains.

* Corresponding author; e-mail tardieu@ensam.inra.fr; fax 33–4–99–52–21–16.

Abbreviations: B, base zone, DAI, days after initiation; MB, middle to base zone; MT, middle to tip zone; $p_{S\text{-}G2\text{-}M}$, proportion of cells in phase S-G2-M; *RDR*, relative cell division rate; *RER*, relative expansion rate; T, tip zone; $t_{cycle\ 1}$, $t_{cycle\ 2}$, duration of cell cycle calculated with two different methods.

(Jacobs, 1997). When cell division rate was decreased by mutation (Hemerly et al., 1995) or by chemical treatment (Haber and Foard, 1963), it had no apparent effect on tissue expansion or leaf shape (Smith et al., 1996). In contrast, a synchronized regulation of division and expansion has been observed in other cases. The induction of tissue expansion by the cell wall protein expansin was accompanied by cell division (Fleming et al., 1997), suggesting that the processes are not independent. An increase in cell production in roots was associated with an increase in the tissue expansion rate (Doerner et al., 1996). Temperature changes can induce synchronized changes in the two processes so that cell-size profiles are invariant with growth rate in maize roots (Silk, 1992) and leaves (Ben Haj Salah and Tardieu, 1995).

The objective of this study was to analyze spatially and temporally the processes of cell division and tissue expansion in sunflower (*Helianthus annuus* L.) leaves to contribute to the development of a framework of analysis applying to dicot leaves. This was carried out from initiation of the leaf on the apex to completion of cell division and of expansion in all zones of leaves located at two positions on the stem: leaf 8, which is the first leaf initiated after germination, and leaf 16, which is usually one of the largest leaves of the plant. This analysis was performed on the epidermis, which is considered to drive the expansion of all leaf tissues (Kutschera, 1992). A field study was appropriate for this analysis, because of the large number of leaves (more than 300) that had to be sampled to obtain an acceptable time resolution and number of replicates and because of the severe selection of plants, which was necessary at each date for acceptable homogeneity.

MATERIALS AND METHODS

Plant Culture and Growth Conditions

Sunflower (*Helianthus annuus* L., hybrid Albena) plants were grown in a field near Montpellier (southern France) in 1996. Seeds were sown on April 29 and June 29 at 0.03-m depth with a density of seven plants/m^2. Plants were watered twice a week, and periodic measurements showed that predawn leaf water potential never declined below −0.2 MPa during the studied period. Light was measured continuously using a PPFD sensor (LI-190SB, Li-Cor, Lincoln, NE). Air temperature and RH were measured every 20 s (HMP35A Vaisala Oy, Helsinki, Finland). Leaf temperature was measured with a copper-constantan thermocouple (0.4 mm in diameter) appressed to the underside of the lamina. All data of temperature, PPFD, and RH were averaged and stored every 600 s in a data logger (LTD-CR10 wiring panel, Campbell Scientific, Shepshed, Leicestershire, UK). Environmental conditions during the two experiments are presented in Table I.

Table I. *Environmental conditions during the two experiments*

Means were calculated over the total growth period of the studied leaf. ± SD represents the variability between days of the growth period.

Condition	Second Sowing Date, Leaf 8	First Sowing Date, Leaf 16
Air temperature (°C)		
Day	25.9 ± 1.1	22.1 ± 1.1
Night	17.4 ± 1.1	15.2 ± 1.1
Leaf temperature (°C)	22.2	19.0
Cumulative PAR (mol m^{-2} d^{-1})	50.1	35.6
Photoperiod (h)	15.0	14.0

Growth Measurement

Three plants were harvested every 2nd d from germination to the end of expansion of leaf 16 and observed after dissection under a stereomicroscope (Wild F8Z, Leica). A leaf was considered initiated when its primordium was visible (about 40 μm long, Fig. 1A) on the apical meristem with the microscope at magnification ×80. Leaf age was then calculated in DAI. Areas of three leaves, 8 (second sowing date) or 16 (first sowing date), were measured every 2nd d from initiation to emergence by dissecting the apex under the microscope, excising the studied leaf (Fig. 1B), and measuring its area with an image analyzer (model V 4.10, Bioscan-Optimas, Edmonds, WA). When the leaf was 25 mm long (Fig. 1C), it was marked with a stamp and India ink, which drew a regular grid of 70 points used to triangulate the surface into 100 elements (Fig. 2A). Five leaves were photographed with a video camera every day at 12 noon (solar time) during the expansion period, and areas were determined with the image analyzer. Each picture was calibrated with a mark of known length on the leaf. A preliminary experiment (not shown) revealed that printing did not affect leaf expansion rate.

Cell area in the adaxial epidermis of three leaves was measured every 2nd d from five DAI until the end of leaf expansion. A transparent negative film of the adaxial epidermis was obtained after evaporation of a varnish spread on the upper face of the leaf. Films were placed under a microscope (Leitz DM RB, Leica) coupled to the image analyzer. The areas of 50 epidermal cells were measured in three to eight (depending on leaf length) transects perpendicular to the midrib and labeled by their y coordinates (Fig. 2B). During the period from initiation to emergence films were made on the leaves, which were harvested for determination of leaf area. Because leaf area was measured with a nondestructive method after leaf emergence, three leaves were sampled every 2nd d for determination of cell area. Films were obtained in T , MT, MB, and B (Fig. 2A) plus, when necessary, in other transects. The distribution of cell area in each transect was characterized by the mean, variance, and skewness. The latter is an indicator of the asymmetry of the cell area distribution and is calculated as the third-order momentum, taking into account the mean cell area ($\bar{x}$) and the number of cells (n):

$$S = \Sigma(x - \bar{x})^3/n \quad (1)$$

Flow Cytometry

Ten to 20 leaves in positions 8 or 16 on the stem were collected at 6 AM and were dissected into three areas cor-

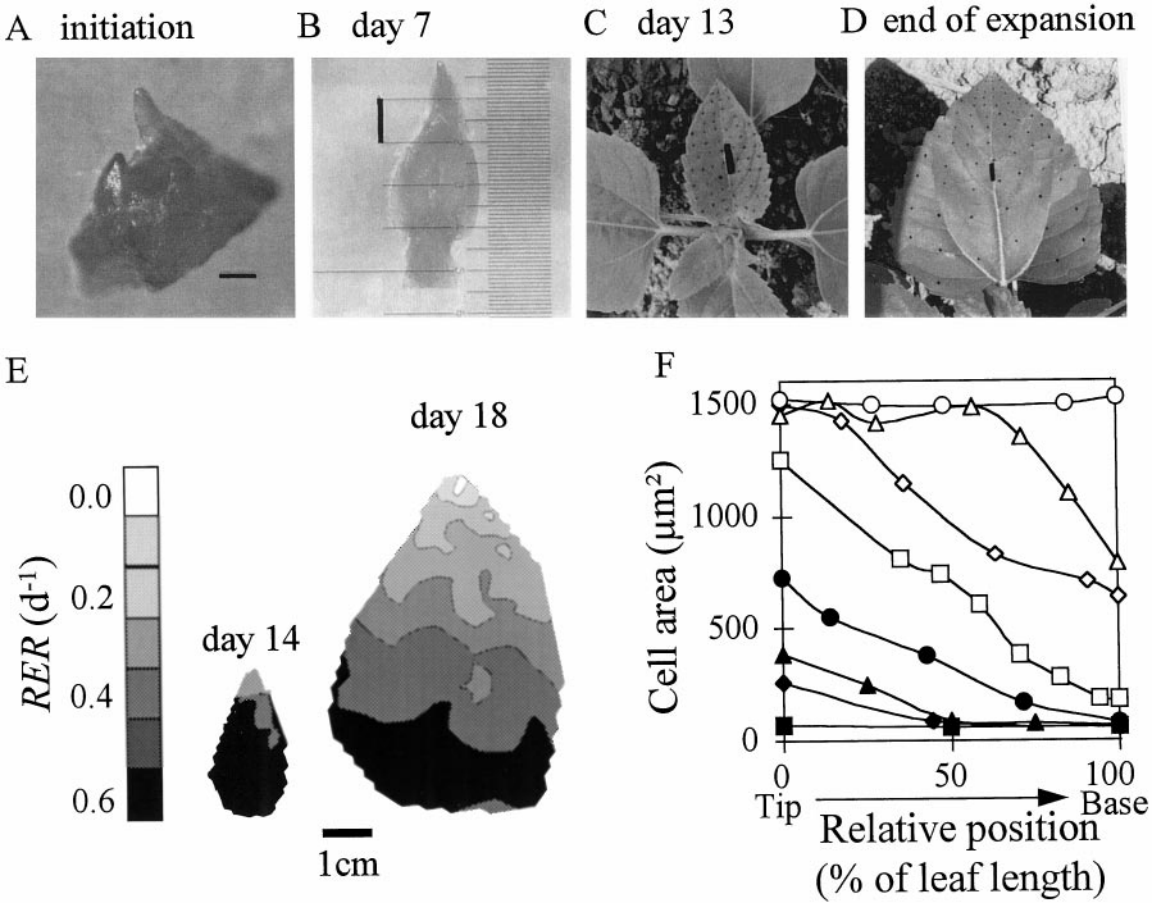

Figure 1. Spatial and temporal changes in morphology and in expansion of leaf 8. A to D, Photographs at the time of initiation on the apex (A, bar = 0.1 mm), on d 7 (B, bar = 1 mm), and 13 (C, bar = 5 mm) after initiation, and at the end of expansion (D, bar = 10 mm). The deformation of the grid of points drawn on the lamina can be seen by comparing C and D. E, Spatial distribution of *RER* calculated in 120 triangles on d 14 (left) and 18 (right). F, Mean cell area as a function of the distance to the leaf tip (expressed as the percentage of total leaf length) on eight dates after initiation: d 9, ■; d 11, ♦; d 13, ▲; d 15, ●; d 17, □; d 19, ◇; d 21, △; and d 23 ○.

responding to B, MB, and MT (Fig. 2A). Leaves 3 or 4, which were mature at the time of sampling, were also collected and prepared in the same way as the studied leaves. Epidermal tissue of each zone was detached with a scalpel and chopped with a razor blade in a plastic Petri dish containing 2 cm^3 of extraction buffer (Dolezel et al., 1989). The suspension obtained was passed through a 50-μm nylon filter and nuclei were stained with 100 mm^3 of propidium iodine (1% in water). Fluorescence intensity of 10,000 nuclei, linked to DNA content, was measured with a FACSCAN-argon laser-flow cytometer (488 nm, 15 mW, Becton Dickinson, Mountain View, CA). Distribution of fluorescence intensity was interpreted as the overlapping of two gaussian curves, the means and SDs of which were calculated (WinMDI Flow cytometry application V1.3.4). This allowed us to calculate the proportion of nuclei with 2c and 4c amounts of DNA. Because mature leaves did not show nuclei with 4c amounts of DNA, it was assumed that there was no endopolyploidy in sunflower leaves. Proportions of nuclei with 2c and 4c were, therefore, interpreted as the proportions of nuclei in phases G0-G1 and G2-M of the cell cycle. Nuclei with intermediate amounts of DNA were considered in phase S. A preliminary experiment, in which leaves were harvested every 6 h for 24 h, tested the influence of time of harvesting on the distribution of nuclei in the cell cycle phases. Because no significant difference in distribution was observed among harvesting times, it was considered that measurements on leaves collected at 6 AM could be considered representative of measurements for the whole day.

Calculations and Spatial Analyses of *RER* and *RDR*

RER of whole leaves ($RER_{leaf,j}$) at time j was calculated from initiation to the end of expansion as the slope (at time j) of the relationship between the logarithm of leaf area (A) and time:

$$RER_{leaf,j} = [d(\ln A)/dt]_j \quad (2)$$

It was calculated by linear regression on the three coupled values of A and t corresponding to times $j - 1$, j, and $j + 1$.

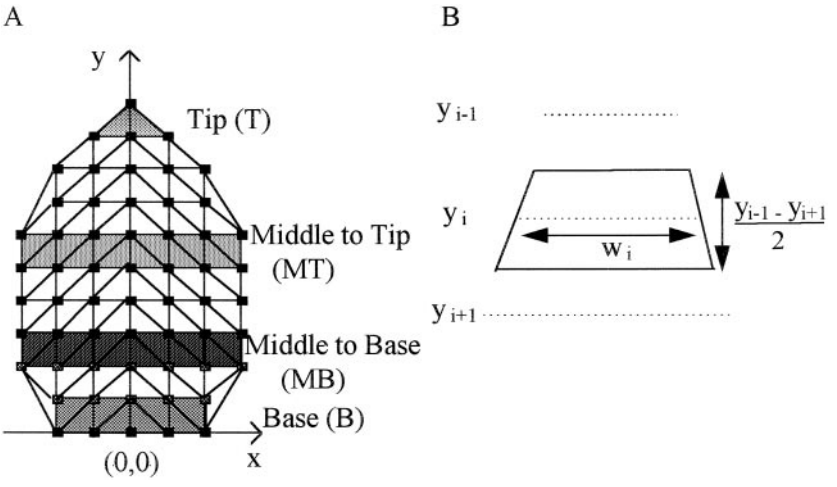

Figure 2. Spatial analyses of *RER* and *RDR* in the leaf. A, Grid of 70 points was drawn on the lamina, defining 120 triangles for calculation of local *RERs*. Coordinates of triangle vertices were defined in a system with the origin at the point of petiole insertion, the *y* axis along the midrib, and the *x* axis perpendicular to it. *RDR* was analyzed in four zones perpendicular to the midrib, T, MT, MB, and B, making up a series of triangles as indicated. B, Calculation of the area corresponding to transect *i*, for calculation of mean cell area per leaf. It was calculated as the area of the trapezoid defined by transects $i - 1$ and $i + 1$, and the edges of the leaf. W_i, Leaf width at the *y* coordinate of transect *i*.

After leaf emergence, spatial analysis of *RER* was carried out using the triangulation. Each triangle was defined by three material points that moved with time in relation to the *x* and *y* axes (Lagrangian approach) but always contained the same cells (plus daughter cells) over time. It was considered that a cell or a material point never crossed the boundaries of the triangle. Coordinates of the triangle vertices were defined daily with respect to a fixed reference system with the origin at the point of petiole insertion, the *y* axis along the midrib, and the *x* axis perpendicular to it. A computer program calculated the area of each triangle and the coordinates of its center of gravity. Local *RER* was estimated in each triangle and attributed to its center of gravity. *RER* of triangle *i* on day *j* ($RER_{i,j}$) was calculated as in Equation 2 by local linear regression taking into account the area of triangle *i* (A_i) at times $j - 1$, *j*, and $j + 1$:

$$RER_{i,j} = [d(\ln A_i)/dt]_j \quad (3)$$

Spatial distribution of $RER_{i,j}$ in the leaf was analyzed by two-dimensional interpolation using a commercial package (Surfer, Golden Software, Inc., Golden, CO; Fig. 1E). For better precision, areas of triangles with common *y* coordinates were pooled, when necessary, for calculation of *RER*s in four zones perpendicular to the midrib (T, MT, MB, and B, Fig. 2A).

Cell number in the same four zones was calculated as the ratio of zone area to mean cell area in the zone, after correction for the number of stomata. $RDR_{i,j}$ in zone *i* and time *j* was calculated by local linear regression taking into account the numbers of cells in zone *i* (N_i) at times $j - 1$, *j*, and $j + 1$:

$$RDR_{i,j} = [d(\ln N_i)/dt]_j \quad (4)$$

Cell number in the whole leaf was estimated by first calculating the mean cell area in each transect drawn on the lamina (Fig. 1F). The proportion of leaf area corresponding to each transect was then calculated as the area of a trapezoid, the sides of which are leaf edges, and lines located at the midpoint between transects (Fig. 2B):

$$A_{ij} = W_{i,j}*(y_{i+1,j} - y_{i-1,j})/2 \quad (5)$$

where $W_{i,j}$ is the leaf width at the *y* coordinate of transect *i* on day *j*, and y_{i-1} and y_{i+1} are *y* coordinates of transects $i - 1$ and $i + 1$ on day *j*. Cell number of the leaf on day *j* ($N_{leaf,j}$) was calculated as:

$$N_{leaf,j} = \Sigma A_{i,j}/a_{ij} \quad (6)$$

where a_{ij} is the mean cell area in transect *i* on day *j*. Summation was carried out over all of the transects analyzed on day *j*. *RDR* of the whole leaf on day *j* ($RDR_{leaf,j}$) was calculated as:

$$RDR_{leaf,j} = [d(\ln N_{leaf})/dt]_j \quad (7)$$

taking into account N_{leaf} on days $j - 1$, *j*, and $j + 1$ in the same way as in Equation 4.

Cell Cycle and Phase S-G2-M durations

Cycle duration in an asynchronous population of cells can be viewed in two ways (Green and Bauer, 1977): either as the "cell-doubling time" required for a population of cells at time *j* to double in number, or as the time that would be required for the "mean" cell of the population at time *j* to complete its cycle if *RDR* did not change with time. Both views are equivalent while an increase in cell number is exponential, i.e. while *RDR* is constant. It follows from Equation 4 that

$$t_{cycle} = \ln(2)/RDR_j \quad (8)$$

In contrast, the views diverge when *RDR* decreases with time. Cell cycle duration calculated at time *j* in the second view ($t_{cycle\ 2j}$) represents an ideal cycle duration that would apply if RDR_j remained constant with time, i.e. if the increase in cell number went back to exponential with the *RDR* observed at time *j*. It is a projection of the duration that a mean cell would spend in the cycle if the latter was in steady state, independent of events that occur after time

j. Under this hypothesis cycle duration at time *j* is

$$t_{\text{cycle 2j}} = \ln(2)/RDR_{\text{j}} \quad (9)$$

thereby increasing with time as RDR_{j} decreases.

In contrast, cell cycle duration calculated at time *j* in the first view ($t_{\text{cycle 1j}}$) is the time required to double $N_{\text{leaf,j}}$ by following the curve relating cell number to time (N[t]). It therefore represents the average cell cycle duration for a cell that begins its cycle at time *j*. If *RDR* decreases linearly with time (Fig. 4, C and D) after it ceases to be constant, the differential equation for $N(t)$ is

$$dN/Ndt = -at + RDR_0 \quad (10)$$

where $-a$ is the slope of the decrease of *RDR* with time and RDR_0 is the constant value of *RDR* during the first (exponential) part of the curve $N(t)$. The solution of $N(t)$ during the second (nonexponential) part of the curve, calculated from Equation 10 is

$$N(t) = N_0 \exp(RDR_0\, t - 0.5at^2) \quad (11)$$

if N_0 is the cell number when *RDR* ceases to be constant and t is 0 at that time. Equation 11 implies that $t_{\text{cycle 1j}}$ is the solution of

$$0.5a(t_{\text{cycle 1j}})^2 - (RDR_0 - at)*t_{\text{cycle 1j}} + \ln(2) = 0 \quad (12)$$

indicating that $t_{\text{cycle 1j}}$ is a function of t and that Equation 10 may have no solution in some cases. Cell cycle duration calculated in this view depends on changes in *RDR* that occur after time *j*.

Duration of phases of the cell cycle was calculated by considering the view corresponding to Equation 9, because it depends on proportions of cells in each phase at time *j*, regardless of events that may occur afterward. At that time, cell cycle is considered as being at instantaneous steady state in each zone of the leaf (see arguments for this hypothesis in "Discussion"). The duration of a given phase at time *j* is proportional to the frequency of cells in this phase at the same time. Duration of a phase can therefore be calculated as the product of the percentage of cells in this phase (estimated by flow cytometry) by $t_{\text{cycle 2}}$ at time *j*. Because of the lack of precision of flow cytometry when 10,000 nuclei only are counted, only two phases were considered, G0-G1 and S-G2-M. The duration of the S-G2-M phase ($t_{\text{S-G2-M,j}}$) was therefore calculated as

$$t_{\text{S-G2-M,j}} = t_{\text{cycle 2j}} * p_{\text{S-G2-M,j}} \quad (13)$$

where $p_{\text{S-G2-M,j}}$ is the frequency of cells in phases S, G2, and M at time *j*. The duration of the G0-G1 phase was calculated in the same way.

RESULTS

Leaf expansion occurred for more than 27 d in leaf 8 (Fig. 3A), from initiation on the apex to the end of expansion, and for more than 35 d in leaf 16 (Fig. 3B). The expansion rate was less than 100 $mm^2\ d^{-1}$ during the first 13 and 20 DAI in leaves 8 and 16, respectively, with an exponential relationship between leaf area and time (nearly constant *RER*, Fig. 3, C and D). In leaf 8 the expansion rate increased rapidly after d 13 (e.g. 2,000 $mm^2\ d^{-1}$ on d 20) and slowed after d 23. *RER* remained constant until d 13 and decreased afterward (Fig. 3C). The pattern of leaf development was similar in leaf 16 with a larger final leaf area (30,000 versus 18,000 mm^2, Fig. 3, A and B) in spite of a slightly slower *RER* (0.51 versus 0.62 d^{-1}, Fig. 3, C and D). Therefore, the greater final area in leaf 16 resulted from the longer duration of expansion.

RER was highly nonuniform in the leaf, with a variability linked to time and to the distance to the leaf tip (Fig. 1E). In the period from 13 to 15 DAI, *RER* in leaf 8 was uniform in the whole leaf except in the tip (Fig. 1E, left), with values in MT, MB, and B close to that calculated in the whole leaf at the beginning of expansion (Fig. 3C). *RER* began to decrease on d 16, 17, and 18, respectively, in MT, MB, and B, whereas it had already decreased on d 13 in T (Fig. 3C). The gradient of *RER* on d 18 was therefore shifted toward the base of the leaf in comparison to d 13 (Fig. 1E, right). The sequence of events was similar in leaf 16 but with a longer period with constant *RER*, which began to decrease on d 20, 24, 27, and 29 in T, MT, MB, and B (Fig. 3D). Because slowing of expansion occurred with a gradient essentially parallel to the midrib, triangles at the leaf base had a final area greater than those at the tip. This resulted in larger final areas of zones toward the base of the leaf (final zone areas of 50, 450, 1400, and 2800 mm^2 in T, MT, MB, and B, respectively, in leaf 8, Fig. 3A), which contributed to the characteristic shape of the leaf (Fig. 1D), in addition to the anisotropy of expansion described by Erickson (1966).

Cell division occurred over 21 and 32 d, respectively, in leaves 8 and 16 (Fig. 4, A and B), i.e. over 78 and 90% of the total duration of leaf expansion. Division rate was slower in leaf 16 than in leaf 8 during the exponential phase (*RDR* of 0.40 versus 0.57 d^{-1}). Therefore, the greater final cell number in leaf 16 (34×10^6 compared with 12×10^6 epidermal cells in leaf 8) was due to the longer duration of cell division. In leaf 16 *RDR* remained nearly constant for 20 d in the whole leaf (Fig. 4D). It decreased first at the T and then in MT, MB, and B. It is noteworthy that an increase in cell number was still exponential in B on d 23, whereas division ceased on d 32. Steep *RDR* decreases were also observed in the other three zones. The time during which cells divided with a nonexponential increase was therefore short compared with the total duration with cell division (7 versus 32 d). The same pattern applied to leaf 8, with a shorter period (13 d) with constant *RDR* (Fig. 4C) and, in B, a delay of 5 d between the end of exponential increase in cell number and the end of division.

At each time, *RER* was greater than *RDR*; therefore, cell area increased with time for the whole development period (Fig. 5). Rapid increase in cell area was simultaneous in each zone with the slowing of *RDR*, which occurred 3 to 5 d before that of *RER*. No gradient of cell area was observed in leaf 8 until d 9 (Fig. 1F), consistent with a hypothesis that both *RDR* and *RER* were uniform in the leaf. At that time, the frequency distribution of cell area was normal, both in the whole leaf and in the base of the leaf (Fig. 6, A and D, skewness = 0.8×10^4 and 1×10^4, respectively). When *RDR* began to decrease in the tip (11 DAI), cells located

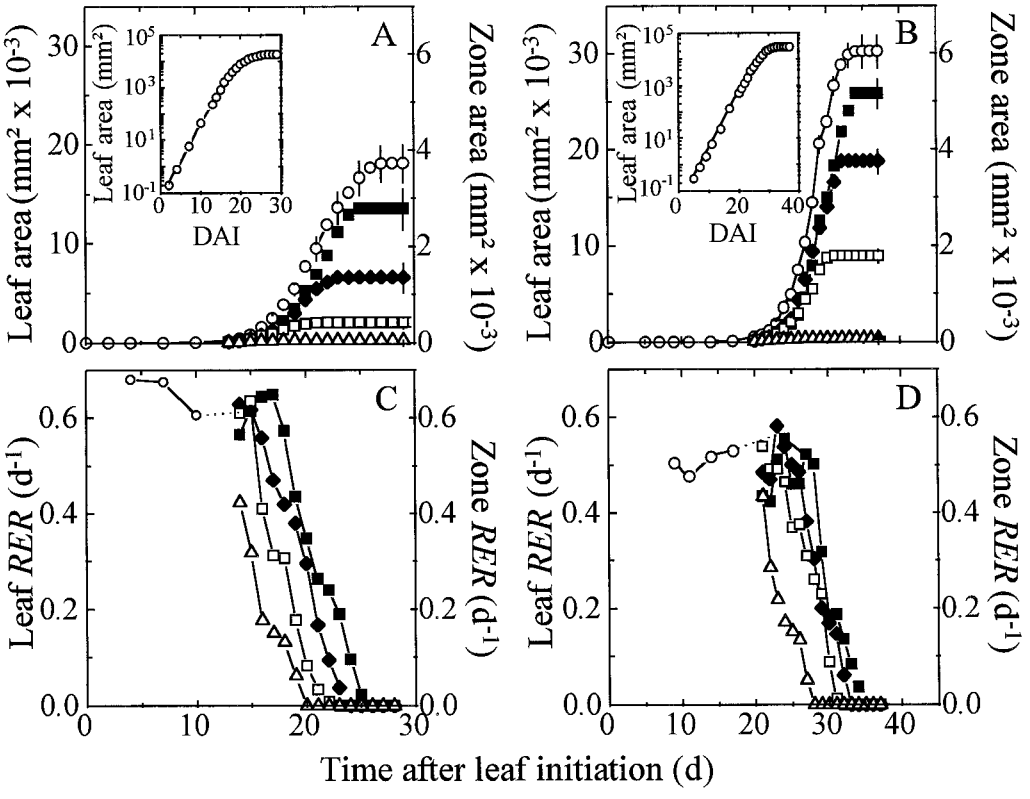

Figure 3. Change with time in the area of the whole leaf and of zones drawn on the lamina of leaves 8 (A) and 16 (B). Corresponding changes with time in *RER* in the whole leaf and in the leaf zones are shown in C and D. Insets, Logarithmic representations of changes with time in leaf area for leaves 8 (A) and 16 (B). Symbols represent either the whole leaf (○) or one of the four zones, B (■), MB (◆), MT (□), and T(△), as shown in Figure 2. For better legibility, intervals of confidence at 0.95 are presented every 2nd d for the whole leaf or at the end of expansion for each zone. Whole-leaf *RER* is shown only during the period while leaf expansion is exponential. Dotted lines link *RER* of the whole leaf at the end of this period to the first measured *RER* in B.

near the tip had a rapid increase in area and were 7 times larger than those in the base on d 17. Consequently, the frequency distribution of cell area in the whole leaf was more and more skewed (Fig. 6, B and C, skewness = 1.1×10^7 and 2.6×10^8), whereas it remained normal (skewness = 7×10^4 and 3.4×10^4) in each individual zone (Fig. 6, E and F). Tissue expansion in a zone ceased when cell area in this zone reached 1500 μm^2 for leaf 8 and 930 μm^2 for leaf 16 (Fig. 5). Consequently, the gradient of cell area in leaf 8 flattened from d 12 onward, i.e. when cells more and more distal to the tip reached 1500 μm^2 (Fig. 1F). That cell area was the same in all zones was accounted for by the same relation between cell division and expansion in all of the zones.

Cell cycle durations were 1.3 and 1.7 d in leaves 8 and 16, respectively, during the period with exponential increase in cell number (Eq. 8). Afterward, cycle duration increased rapidly with a tip-to-base gradient that followed that of cell division rate (Fig. 7, A and B). Calculated with Equation 9, $t_{cycle\ 2}$ in B reached 13 d on d 19, i.e. only 2 d before cessation of division (see oblique dotted line in Fig. 7A). This suggests that the mean cell in B could not complete its cycle after d 19. A similar trend was observed in the base of leaf 16 ($t_{cycle\ 2j}$ of 6.3 d on d 29, i.e. 3 d before the end of division) and in other zones of both leaves. A mean cell of the considered zone could not complete its cycle after 4 d beyond the end of exponential increase in cell number. The same conclusion was drawn for the other three zones (Table II). Calculations carried out with $t_{cycle\ 1j}$ yielded still shorter delays (2 d) between the end of exponential increase and the time when Equation 12 had no solution, suggesting that a cell that began its cycle slightly after the end of exponential increase could not finish its cycle.

In each zone the proportion of nuclei in the S-G2-M phase declined, cell cycle duration increased (Fig. 7, C and D), and a tip-to-base gradient was observed at each date. The decrease in $p_{S\text{-}G2\text{-}M}$ compensated for the increase in cell cycle duration; therefore, the duration of the S-G2-M phase, as calculated by Equation 13, remained in a narrow range (0.1–0.4 d) at all times in all zones and leaves being studied (Fig. 7, E and F). This suggests that the considerable increase with time in $t_{cycle\ 2j}$ was essentially due to an increase in duration of G0-G1. The proportion of cells in the S-G2-M phase decreased as more cells were blocked in the G0-G1 phase, reaching 0 when cell division ceased, but the duration of this phase did not substantially change with time.

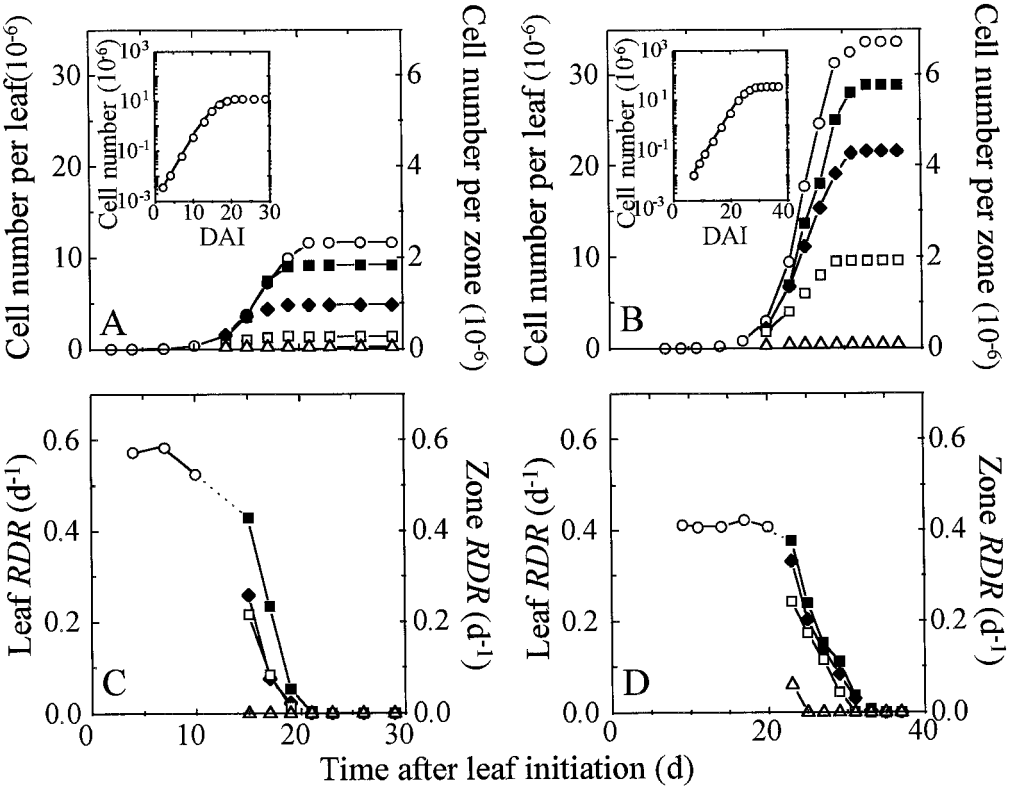

Figure 4. Change with time in epidermal cell number in the whole leaf and in zones drawn on the lamina of leaves 8 (A) and 16 (B). Corresponding changes with time in *RDR* in the whole leaf and in the leaf zones are shown in C and D. Insets, Logarithmic representation of change with time in leaf cell number for leaves 8 (A) and 16 (B). For better legibility, leaf *RDR* is shown only during the period while cell division is exponential. Symbols are as in Figure 3.

DISCUSSION

Changes with time in *RDR* and *RER* followed a common pattern, with constant values for more than one-half of the leaf development period and with a rapid decline with time afterward. This pattern, although essentially similar to that described for whole-leaf *RDR* by Dale (1964) and Milthorpe and Newton (1963) and for whole-leaf *RER* by Denne (1966), Hannam (1968), and Poethig and Sussex (1985), differs from published data in two ways: (a) Although we confirm that, studied at the whole-leaf level, the time during which *RDR* and *RER* were declining represented an appreciable proportion of the total duration of development, declines were short (less than 25% of the total duration of division) in each individual zone. Discrepancy between analyses in the whole leaf and in each zone were due to the fact that the decline in *RER* or *RDR* began in the whole leaf on the day when it began in the tip and ended on the day when it ended in the base. Duration of decline was therefore longer and overall rate was slower in the whole leaf than in each zone. (b) We show that *RDR* and *RER* underwent parallel changes, with common values for each in all zones of the leaf at the beginning of development and a decline of *RER* that lagged behind that of *RDR* in all zones. Durations and rates of decline were similar in all zones of a leaf, so that the only difference among zones was the timing of onset of decline of *RER* or *RDR*. This is in opposition to the conclusion of Poethig and Sussex (1985), who stated that the ovate shape of the tobacco leaf was due to a larger *RER* in the basal region of the leaf.

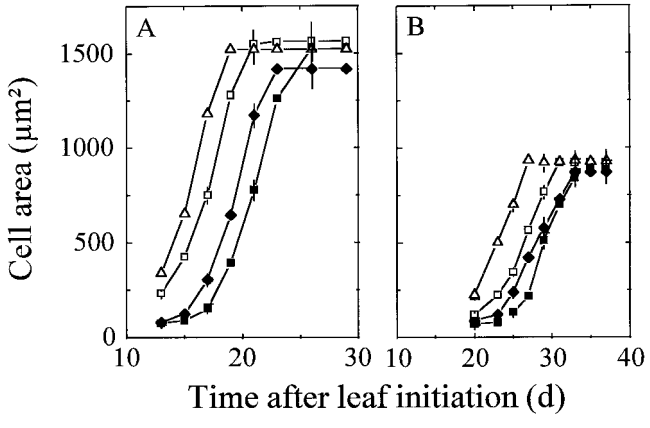

Figure 5. Change with time in epidermal cell area in zones of leaves 8 (A) and 16 (B). Symbols are as in Figure 3. Intervals of confidence at 0.95 are presented every 2nd d for better legibility.

Our results cast doubt on the possibility that a decline in the cell division rate could be triggered by an increase in cell area, since similar *RDRs* were observed at the beginning and at the end of the period with an exponential increase in cell number, in spite of different cell areas

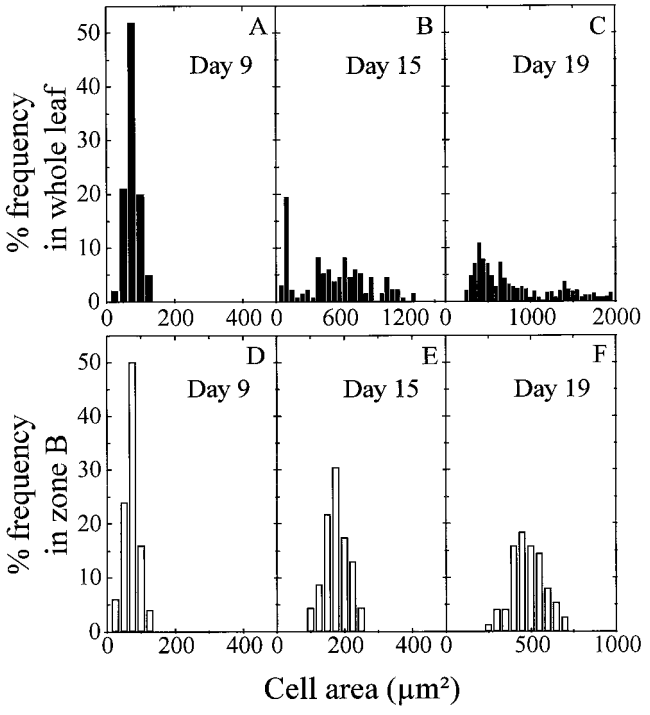

Figure 6. Frequency distribution of epidermal cell area in leaf 8 on d 9 or after the period with exponential increase in cell number (d 15 and 19 after initiation). A to C present the frequency distribution analyzed over the whole leaf. D to F present that analyzed in zone B only. Note that scales of *x* axes differ among the panels.

(80–200 μm^2). Following Green's (1976) framework of analysis, change in relative cell expansion rate results from the difference between *RER* and *RDR*. During the period with constancy of both *RDR* and *RER*, cell area increased with time, because *RER* was higher than *RDR*. As in the theory of control by size, *RDR* declined in all zones when cell area began to increase rapidly. Our results suggest that this may be due to the existence of a transition period during which *RER* was maintained after *RDR* began to decline. In this view, the rapid increase in cell area might be a consequence of the decline in *RDR* rather than the cause of this decline.

The decrease in *RDR* after a period of constancy has been interpreted either as a consequence of the fact that an increasing proportion of cells left the cell cycle (Dale, 1970) or that the duration of the cycle increased simultaneously in all cells (Nougarède and Rondet, 1976). In the first case, one could expect that cells that leave the cycle would have a faster increase in area than cells still in the cycle (Green, 1980), because they would have a maintained *RER* with null *RDR*. Repeated over several days, this process would lead to a nonsymmetrical distribution of cell area. Such a skewed distribution was observed over the whole leaf when division began to slow in the tip (Fig. 6, B and C; Pyke et al., 1991). It was not observed within each zone where the whole histogram of cell area remained normal and moved toward higher values without appreciable increase in variance or in skewness. This result indicates that the first hypothesis was correct in the case of sunflower leaves but did not apply randomly in the leaf. Departure from the cell cycle occurred following a tip-to-base gradient, but no early departure from the cell cycle could be detected within a given zone of the leaf, since cell area distribution remained normal until the end of cell division.

Here we propose two modes of calculation of cell-cycle duration, which either overestimate ($t_{cycle\ 1}$) or underestimate ($t_{cycle\ 2}$) this duration during the time that the *RDR* declines. The classical method of estimation ($t_{cycle\ 2}$, Eq. 9) underestimates cycle duration because it assumes that increase in cell number goes back to exponential and that cell cycle goes back to steady state. In contrast, $t_{cycle\ 1}$ overestimates cycle duration because it considers a cell that would begin its cycle on the studied day and not a mean cell of the population. It is interesting to note that both calculations lead to similar results, i.e. that cells stop somewhere in the cycle very soon (2–4 d, depending on the zone and the mode of calculation) after the end of steady state in the cycle.

A calculation was also proposed to evaluate in situ the times elapsed in phases S-G2-M and G0-G1. This calculation is correct while the cell cycle is in steady state, i.e. during exponential increase in cell number (Green and Bauer, 1977). Durations of phases calculated here are consistent with direct measurements based on the use of [^{3}H]thymidine or colchicine treatments combined with Feulgen microdensitometry in the apical meristem of *Chrysanthemum segetum* (Nougarède and Rondet, 1978). This group found a low variability of the S-G2-M phase (7–8 h), whereas the whole cycle increased in duration from 51 to 135 h. In the same way, an increase in phase G0-G1 duration, when the cell cycle slows, was observed by Nougarède and Rembur (1985) and Francis (1992).

In spite of likely errors on individual calculations of t_{cycle} and $t_{S\text{-}G2\text{-}M}$, consistent tendencies can be drawn independently of methods of calculation, zone in the leaf, and leaf position on the stem. A short delay elapsed between the end of steady state in the cell cycle and the time when studied cells could no longer complete their cycle. This suggests that decline with time in cell division rate was not linked to a steady increase in cycle duration but to a blockage of some step in the cycle. Limiting steps classically described (Francis, 1992) are those between phases G1 and S and between phases G2 and M. The second possibility is not supported by our in situ evaluation. If cells were blocked in the G2 phase, the proportion of cells in the S-G2-M phase would increase with time as *RDR* decreases, whereas the opposite tendency was observed. The first possibility is also difficult to reconcile with our data. If cells were abruptly blocked at the transition between phases G1 and S on the day when the cell cycle ceased to be in steady state, cell division would end in 3 to 6 h (necessary time for the depletion of the existing stock of cells in the S-G2-M phase). One can imagine either that cells were blocked somewhere in the early G1 phase or that a decreasing proportion of cells could cross the G1-S phase transition. In any case, this would lead to an increase with time in the G0-G1 phase mean duration and to the reduction in proportion of cells in phase S-G2-M, as experimentally observed. One hypothesis for the loss of competence of cells to divide in the leaf is the inactivation of cdc2 (Martinez et

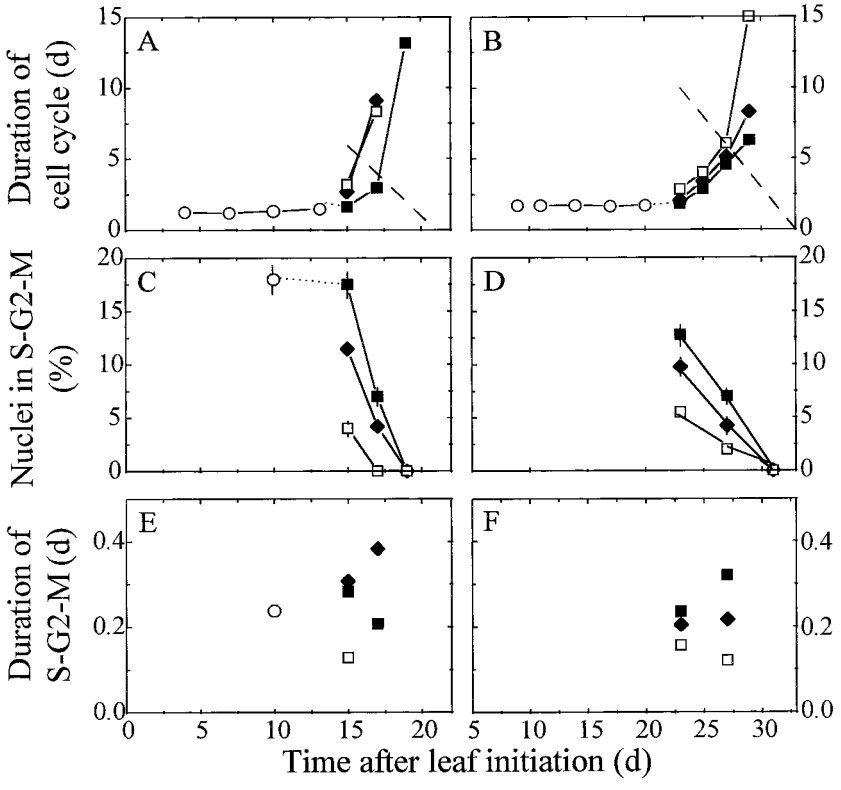

Figure 7. In situ analysis of cell cycle. A and B show changes with time in the duration of the cell cycle, as calculated in Equation 9, in leaves 8 (left) and 16 (right) and in zones drawn on the lamina of both leaves. C and D show changes with time in the percentage of nuclei in the S-G2-M phase analyzed by flow cytometry. E and F show changes with time in the duration of the S-G2-M phase as calculated in Equation 13. Symbols are as in Figure 3. The oblique dotted lines in A and B represent the times that remain available before completion of division in the base of the leaf. When duration of the cell cycle exceeds this limit, a mean cell in zone B will not have time to complete its cycle. Intervals of confidence at 0.95 are presented for flow-cytometry data.

al., 1992) by the changes in metabolic status occurring during the sink-to-source transition within the leaf (Turgeon and Webb, 1973). Changes in carbon status have been shown to be accompanied by changes in *RDR* in maize roots (Muller et al., 1998). Suc starvation, for example, is known to cause an accumulation of root cells in the G1 phase (Van't Hof, 1973).

An intriguing result was that final cell area was common to all zones of a leaf, in spite of different timings of events from the tip to the base. In all zones of a given leaf, *RER* reached 0 when this maximum cell area was reached. This could not be due to a genetic control of cell size, because final areas differed in leaves 8 and 16 analyzed here, but also in a series of similar analyses carried out in the field and in the greenhouse (C. Granier and F. Tardieu, unpublished data). Change in final cell area with position on the stem was also observed by Ashby (1948). Common final cell area was probably due to the fact that changes in *RER* and *RDR* were strictly parallel in all zones of a leaf, but the period with maintained *RER* and declining *RDR* was shorter in leaf 16 than in leaf 8. Underlying mechanisms of control remain to be investigated.

Lower *RER* and *RDR* in leaf 16 were probably due to a lower leaf temperature during the development of leaf 16 (Table I). As in the case of maize (Ben Haj Salah and Tardieu, 1995), rates of expansion and of division are linearly related to temperature with an x intercept of approximately 5°C (C. Granier and F. Tardieu, unpublished data) and can therefore be expressed in thermal time. *RER* of leaves 8 and 16 were similar if expressed in thermal time with a base of 5°C (0.036 and 0.035°C d^{-1}), and the same conclusion applied to *RDR* (0.032 and 0.030°C d^{-1}).

Table II. *Durations of the periods with constant RDR (exponential increase in cell no.) in zones B, MB, and MT of leaves 8 and 16; durations of periods during which a cell that begins its cycle can complete it before the end of division, if calculated with Equation 12 ($t_{cycle\ 1}$); durations of periods during which a mean cell can complete its cycle before the end of division, if calculated with Equation 9 ($t_{cycle\ 2}$)*

Durations	Leaf 8			Leaf 16		
	B	MB	MT	B	MB	MT
			d			
Period with constant *RDR*	13	11	9	23	21	19
Period with completion of cell cycle, $t_{cycle\ 1}$	15	13	11	25	23	21
Period with completion of cell cycle, $t_{cycle\ 2}$	17	15	13	27	25	23

CONCLUSION

Leaf area and cell number increased exponentially during most of the duration of leaf development, with uniform values of *RDR* and *RER* in the whole leaf during this period. Cessation of cell division occurred abruptly in a given zone of the leaf, with cells blocked in the G0-G1 phase of the cycle, followed after a few days by cessation of expansion. This pattern was common to all zones of a leaf and to leaves located at two positions on the stem. Because of parallelisms of decreases in *RDR* and *RER* in all zones,

final cell area was uniform in a leaf but not among leaves located at different positions on the stem. Uniformity of final cell area in spite of lagged sequences of events was, therefore, due to the coordination between division and expansion processes and not by a direct genetic control of cell area. Results regarding cell cycle suggest that decrease with time in cell division rate should be viewed as an abrupt loss of competence of cells at a critical step rather than a gradual slowing of the cycle. Overall, the results suggest that spatial variability of development among zones of a leaf and among leaves of a plant can be regarded with a simple framework, where gradients and differences among leaves essentially depend on the occurrence of two events, cessation of exponential expansion and of exponential division. In contrast, rates of processes seemed to be well conserved within a leaf and, probably, among leaves of a plant.

ACKNOWLEDGMENTS

The authors thank Philippe Barrieu for technical assistance during flow-cytometry experiments, André Bouchier for programmation of triangles area, and Dr. Michaux-Ferriere (Centre de Cooperation Internationale en Recherche Agronomique pour le Development) for helpful discussions about flow-cytometry data.

Received June 30, 1997; accepted November 19, 1997.

LITERATURE CITED

Ashby E (1948) Studies in the morphogenesis of leaves. 2. The area, cell size and cell number of leaves of Ipomoea in relation to their position on the shoot. New Phytol **47:** 177–195

Avery GS (1933) Structure and development of the tobacco leaf. Am J Bot **20:** 565–591

Ben Haj Salah H, Tardieu F (1995) Temperature affects expansion rate of maize leaves without change in spatial distribution of cell length. Analysis of the coordination between cell division and cell expansion. Plant Physiol **109:** 861–870

Dale JE (1964) Leaf growth in *Phaseolus vulgaris*. I. Growth of the first pair of leaves under constant conditions. Ann Bot **28:** 579–589

Dale JE (1970) Models of cell number increase in developing leaves. Ann Bot **34:** 267–273

Denne P (1966) Leaf development in *Trifolium repens*. Bot Gaz **127:** 202–210

Doerner P, Jorgensen JE, You R, Steppuhn J, Lamb C (1996) Control of root growth and development by cyclin expression. Nature **380:** 520–523

Dolezel J, Binarova P, Lucretti S (1989) Analysis of nuclear DNA content in plant cells by flow cytometry. Biol Plant **31:** 113–120

Erickson RO (1966) Relative elemental rates and anisotropy of growth in area: a computer programme. J Exp Bot **17:** 390–403

Fleming AJ, McQueen-Mason S, Mandel T, Kuhlemeir C (1997) Induction of leaf primordia by the cell wall protein expansin. Science **276:** 1415–1418

Francis D (1992) The cell cycle in plant development. New Phytol **122:** 1–20

Fraser TE, Silk WK, Rost TL (1990) Effects of low water potential on cortical cell length in growing regions of maize roots. Plant Physiol **93:** 648–651

Gandar PW, Hall AJ (1988) Estimating position-time relationships in steady-state one-dimensional growth zones. Planta **175:** 121–129

Green PB (1976) Growth and cell pattern formation on an axis: critique of concepts, terminology, and mode of study. Bot Gaz **137:** 187–202

Green PB (1980) Organogenesis—a biophysical view. Annu Rev Plant Physiol **31:** 51–82

Green PB, Bauer K (1977) Analyzing the changing cell cycle. J Theor Biol **68:** 299–315

Haber AH, Foard DE (1963) Nonessentiality of concurrent cell divisions for degree of polarization of leaf growth. II. Evidence from untreated plants and from chemically induced changes of the degree of polarization. Am J Bot **50:** 937–943

Hannam RV (1968) Leaf growth and development in the young tobacco plant. Aust J Biol Sci **21:** 855–870

Hemerly A, Almeida Engler J, Bergounioux C, Van Montagu M, Engler G, Inzé D, Ferreira P (1995) Dominant negative mutants of the Cdc2 kinase uncouple cell division from iterative plant development. EMBO J **14:** 3925–3936

Jacobs T (1997) Why do plant cells divide? Plant Cell **9:** 1021–1029

Kutschera U (1992) The role of the epidermis in the control of elongation growth in stem and coleoptiles. Bot Acta **105:** 246–252

Lecoeur J, Wery J, Turc O, Tardieu F (1995) Expansion of pea leaves subjected to short water deficit: cell number and cell size are sensitive to stress at different periods of leaf development. J Exp Bot **46:** 1093–1101

Maksymowych R (1973) Cell enlargement and differentiation. *In* Analysis of Leaf Development. Cambridge University Press, Cambridge, UK, pp 50–57

Martinez MC, Jorgensen JE, Lawton MA, Lamb CJ, Doerner P (1992) Spatial pattern of cdc2 expression in relation to meristem activity and cell proliferation during plant development. Proc Natl Acad Sci USA **89:** 7360–7364

Milthorpe FL, Newton P (1963) Studies on the expansion of the leaf surface. III. The influence of radiation on cell division and leaf expansion. J Exp Bot **14:** 483–495

Muller B, Stosser M, Tardieu F (1998) Spatial distributions of tissue expansion and cell division rates are related to PPFD and to sugar content in the growing zone of maize roots. Plant Cell Environ (in press)

Nougarède A, Rembur J (1985) Le point végétatif en tant que modèle pour l'étude du cycle cellulaire et de ses points de contrôle. Bull Soc Bot Fr Actual Bot **132:** 9–34

Nougarède A, Rondet P (1976) Durée des cycles cellulaires du méristème terminal et des méristèmes axillaires du *Pisum sativum* L. C R Acad Sci Paris Ser D **282:** 715–718

Nougarède A, Rondet P (1978) Evénements structuraux et métaboliques dans les entre-noeuds des bourgeons axillaires du pois, en réponse à la levée de dominance. Can J Bot **56:** 1213–1228

Peters WS, Bernstein N (1997) The determination of relative elemental growth rate profiles from segmental growth rates. Plant Physiol **113:** 1395–1404

Poethig RS, Sussex IM (1985) The developmental morphology and growth dynamics of the tobacco leaf. Planta **165:** 158–169

Pyke KA, Marrison JL, Leech RM (1991) Temporal and spatial development of the cells of the expanding first leaf of *Arabidopsis thaliana* (L.) Heynh. J Exp Bot **42:** 1407–1416

Sato Y, Tamaoki M, Murakami T, Yamamoto N, Kano-Murakami Y, Matsuoka M (1996) Abnormal cell division in leaf primordia caused by the expression of the rice homeobox gene OSH1 leads to altered morphology of leaves in transgenic tobacco. Mol Gen Genet **251:** 13–22

Saurer W, Possingham JV (1970) Studies on the growth of spinach leaves (*Spinacea oleracea*). J Exp Bot **21:** 151–158

Sharp RE, Silk WK, Hsiao TC (1988) Growth of the maize primary root at low water potentials. I. Spatial distribution of expansive growth. Plant Physiol **87:** 50–57

Silk WK (1992) Steady form from changing cells. Int J Plant Sci **153:** 49–58

Skinner RH, Nelson CJ (1994) Epidermal cell division and the coordination of leaf and tiller development. Ann Bot **74:** 9–15

Smith LG, Hake S, Sylvester AW (1996) The *tangled-1* mutation alters cell division orientations throughout maize leaf development without altering leaf shape. Development **122:** 481–489

Tsuge T, Tsukaya H, Uchimiya H (1996) Two independent and polarized processes of cell elongation regulate leaf blade expansion in *Arabidopsis thaliana* (L.) Heynh. Development **122:** 1589–1600

Turgeon R, Webb JA (1973) Leaf development and phloem transport in *Cucurbita pepo*: transition from import to export. Planta **113:** 179–191

Van Lijsebettens M, Clarke J, Vanderhaeghen R, Cnops G, De Bleeckere M, Wang X, Beeckman T, Van Montagu M (1996) Genetics aspects of leaf development. *In* J Gielis, T Gerats, eds, Aspects of Morphogenesis of Leaves, Flowers and Somatic Embryos, Vol 13. Scripta Botanica Belgica, Leuven, Belgium, pp 29–39

Van't Hof J (1973)The regulation of cell division in higher plants. Brookhaven Symp Biol **25:** 152–165

Wolf SD, Silk WK, Plant RE (1986) Quantitative patterns of leaf expansion: comparison of normal and malformed leaf growth in *Vitis vinifera* cv. Ruby Red. Am J Bot **73:** 832–846

Yegappan TM, Paton DM, Gates CT, Muller WJ (1980) Water stress in sunflower (*Helianthus annuus* L.). II. Effects on leaf cells and leaf area. Ann Bot **49:** 63–68